Multinucleon Transfer in 25 MeV/nucleon ^{86}Kr + ^{64}Ni, ^{124}Sn Peripheral Collisions

Olga Fasoula[1,*], *Georgios* Souliotis[1], *Stergios* Koulouris[1], *Athena* Pakou[2], *Martin* Veselsky[3], *Sherry* Yennello[4], and *Aldo* Bonasera[4]

[1]Laboratory of Physical Chemistry, Department of Chemistry, National and Kapodistrian University of Athens, Athens, Greece
[2]Department of Physics and HINP, University of Ioannina, Ioannina, Greece
[3]Institute of Experimental and Applied Physics, Czech Technical University, Prague, Czech Republic
[4]Cyclotron Institute, Texas A&M University, College Station, Texas, USA

Abstract. In this work we investigate multinucleon transfer reaction channels in peripheral collisions between a ^{86}Kr projectile at 25 MeV/nucleon with ^{64}Ni and ^{124}Sn targets. The experimental data of these reactions were obtained with the Momentum Achromat Recoil Separator (MARS) at Texas A&M University in previous works of our group. We extracted and compared experimental mass and momentum per nucleon distributions of ejectiles with a two step model calculation. For the interaction of the projectile with the target, the phenomenological Deep Inelastic Transfer model (DIT) and the microscopic Constrained Molecular Dynamics model (CoMD) were used, both followed by the GEMINI model for the de-excitation of the primary excited projectile-like fragments. Generally, both DIT and CoMD appear to describe the trend of the data for both systems. However, possible further improvements in the models may be necessary. In conjunction with our recent work with a ^{86}Kr beam at 15 MeV/nucleon with a ^{64}Ni target, this study provides further insights into the reaction mechanisms of peripheral collisions in the Fermi energy regime and the production of neutron rich nuclides.

1 Introduction

The study of multinucleon transfer reactions (MNT) has been one of the fundamental issues for the nuclear physics community through the years [1, 2]. The importance of these reactions is highlighted by the fact they can be used for the production of neutron rich nuclei far from stability.

Efforts are ongoing in our group toward the study of MNT reactions near and below the Fermi energy (15-25 MeV/nucleon) [3–9]. We previously presented our preliminary work on projectile-like fragment distributions from the reaction of a ^{86}Kr beam at 15 MeV/nucleon with a target of ^{64}Ni by comparing experimental data with model calculations [7]. In this work, we focus on the reactions between a ^{86}Kr beam at 25 MeV/nucleon and targets of ^{64}Ni and ^{124}Sn. We have extracted mass and momentum per nucleon distributions and compare them with model calculations on channels that produce neutron rich nuclei.

The structure of the paper is as follows. In section 2, an overview of the experimental measurements and the data analysis is given. In section 3, a brief introduction of the theoretical models is presented. In section 4, a comparison of the experimental results with the calculations is given, followed by the conclusions in section 5.

2 Experimental Measurements

The experimental data employed in this work were obtained previously with the Momentum Achromat Recoil Separator (MARS) at the Cyclotron Institute at Texas A&M University in two different experiments with a ^{86}Kr^{22+} beam delivered by the K500 Superconducting Cyclotron at 25 MeV/nucleon.

In the first experiment [3], the ^{86}Kr beam impinged on a ^{64}Ni (4 mg/cm^2) target at an angle of 0° and projectile-like fragmnets were collected in the polar angular range $\Delta\theta$ = 1.0° – 2.7° with full azimuthal symmetry resulting in a solid angle of $\Delta\Omega$ = 6.0 msr. In the second experiment [4], the ^{86}Kr beam was sent on a ^{124}Sn (2 mg/cm^2) target at an angle of 4.0° relative to the optical axis of MARS leading to a collection of projectile-like fragments in the polar angular range $\Delta\theta$ = 2.7° – 5.4°. The azimuthal angular acceptance was $\Delta\phi$ = 2.7°, thus defining a solid angle of $\Delta\Omega$ = 2.2 msr. We note that the angular settings lie within the respective grazing angles for these reactions (3.6° for ^{86}Kr + ^{64}Ni and 6.5° for ^{86}Kr + ^{124}Sn). In both experiments the angular ranges correspond to the laboratory reference frame. A series of overlapping magnetic rigidity settings of the separator were performed covering the range Bρ = 1.6 – 2.0 Tm for the ^{86}Kr + ^{64}Ni reaction and Bρ = 1.3 – 2.0 Tm for the ^{86}Kr + ^{124}Sn reaction. Following Bρ – ΔE – E$_r$ (magnetic rigidity, energy-loss, residual-energy)

*e-mail: olgafas@chem.uoa.gr

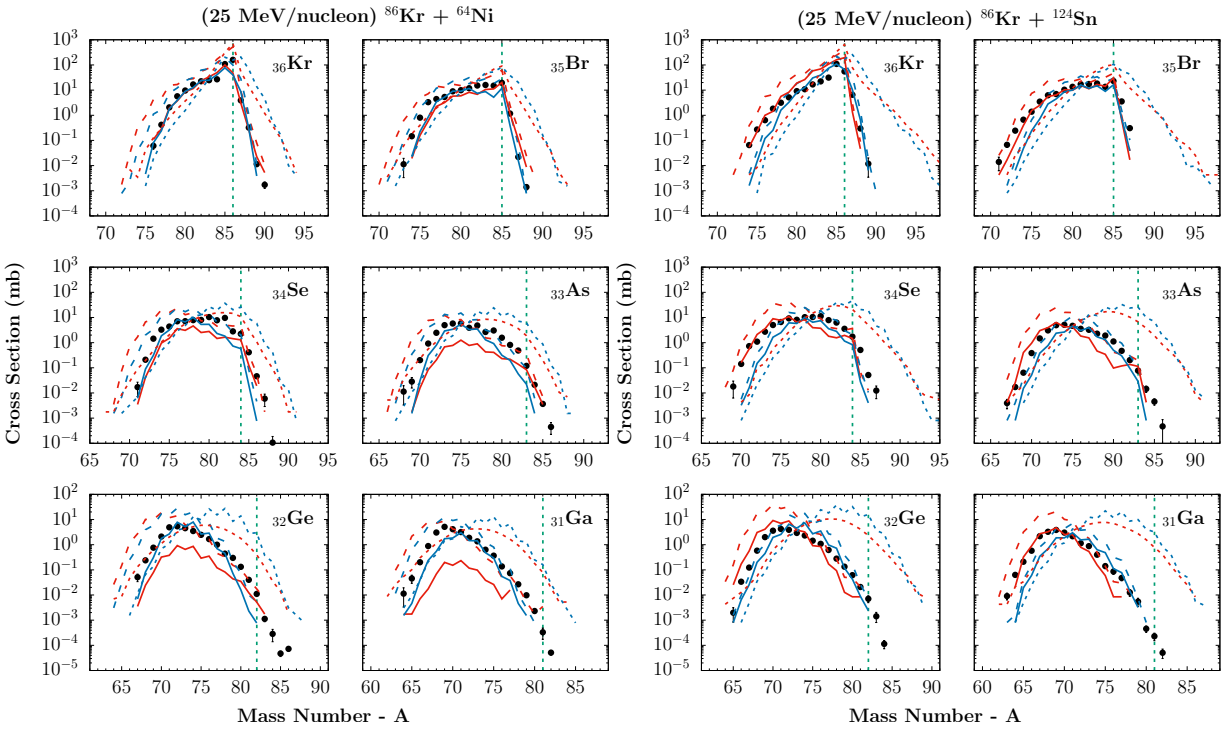

Figure 1. Mass distributions (measured production cross sections) of elements with Z = 31–36 from ^{86}Kr (25 MeV/nucleon) + ^{64}Ni (left) and ^{86}Kr (25 MeV/nucleon) + ^{124}Sn (right). Experimental data: Full (black) circles. DIT calculations: primary fragments: dotted (blue) line, final (cold) fragments: dashed (blue) line, final fragments filtered for acceptance: solid (blue) line. CoMD calculations: primary fragments: dotted (red) line, final (cold) fragments: dashed (red) line, final fragments filtered for acceptance: solid (red) line. The vertical dashed (green) line indicates the initiation of neutron pickup.

and time-of-flight techniques, we obtained high resolution yield distributions with respect to Z, A and velocity from which production cross sections were extracted.

In our previous studies [3, 4], the total production cross sections were obtained from the measured data after corrections for the limited angular acceptance and, subsequently were compared with model calculations. In this work, we focus our study first on the measured yield distributions; furthermore, we continue to extract momentum distributions from the original data and perform detailed comparisons with model calculations expecting to shed light to the reaction mechanisms at this energy regime.

3 Model Calculations

The calculations are based on a two step Monte Carlo approach. The first step is the dynamical part of the reaction, during which the projectile–target interaction takes place, and the second step is the de-excitation of the hot projectile-like and target-like fragments. The dynamical part is simulated either with the phenomenological Deep Inelastic Transfer model (DIT) [10] or with the microscopic Constrained Molecular Dynamics model (CoMD) [11]. The subsequent de-excitation of the produced hot nuclei is performed with the GEMINI model [12]. For the rest of this work, the DIT/GEMINI and CoMD/GEMINI calculations will be referred to as DIT and CoMD calculations, respectively.

4 Results and Comparisons

In this section, we present our model calculations in comparison with experimental mass and momentum per nucleon (p/A) distributions of ejectiles from the reactions of ^{86}Kr + ^{64}Ni and ^{86}Kr + ^{124}Sn at 25 MeV/nucleon.

We keep our focus on reaction channels that produce neutron rich nuclei, namely, proton removal, neutron pickup and multiple charge exchange. We remind that all these data pertain to the ejectiles, as the experimental setup previously described measured the projectile-like fragments of these reactions.

4.1 Mass Distributions

In Fig. 1, we present the yield distributions (measured production cross sections) of the observed isotopes of the elements with Z = 31–36 from the reaction of (25 MeV/nucleon) ^{86}Kr + ^{64}Ni on the left panels and from the the reaction of (25 MeV/nucleon) ^{86}Kr + ^{124}Sn on the right panels. The experimental data are shown by the full black points. The vertical green dashed line denotes the initiation of neutron pickup that develops to the right. We point out that these data are obtained from the measured cross sections in the solid angles $\Delta\Omega$ = 6.0 msr for the ^{86}Kr + ^{64}Ni reaction and $\Delta\Omega$ = 2.2 msr for the ^{86}Kr + ^{124}Sn reaction. We also note that in the Kr + Ni experiment we had full azimuthal coverage, whereas in the Kr + Sn experiment we had partial azimuthal coverage; in this case we multiplied the data by a factor of 9.5 (to obtain azimuthal

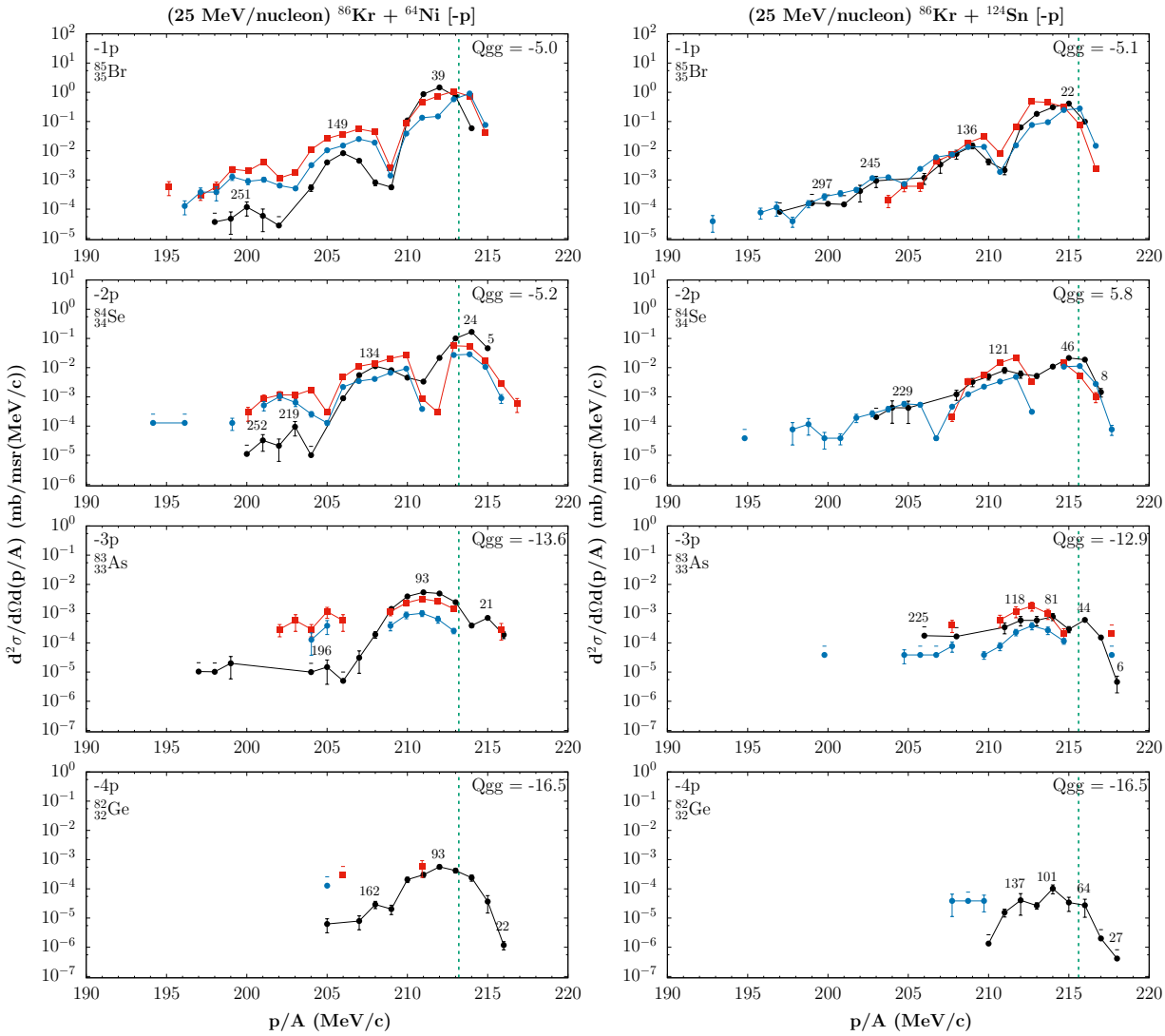

Figure 2. Momentum per nucleon distributions of ejectiles from proton removal channels of (25 MeV/nucleon) ^{86}Kr + ^{64}Ni (left) and (25 MeV/nucleon) ^{86}Kr + ^{124}Sn (right). Experimental data: closed (black) circles. Vertical dashed (green) line: p/A of the beam. Numbers above peaks: total excitation energy of QP–QT system in MeV. Qgg: Ground-to-ground state Q-value in MeV. DIT calculations: closed (blue) circles. CoMD calculations: closed (red) squares.

integration). As we see in Fig. 1, the data from both reactions indicate the production of neutron rich nuclei.

For both reactions, we compare the experimental distributions with three components of the DIT (blue symbols) and CoMD (red symbols) calculations. Dotted lines represent the primary nuclei that after de-excitation lead to "cold" nuclei (that is, nuclei de-excited below the neutron separation energy) presented by dashed lines. These lines in effect represent the entire population of the corresponding nuclides that are produced and could be collected by a spectrometer (or other experimental device) with appropriately large acceptance. In our experiments, the MARS separator has, as we mentioned, a limited angular acceptance and the measurements were performed in a certain magnetic rigidity range. In Fig. 1, the full lines in both calculations depict the cross sections after a filtering process for the polar angular acceptance of MARS and the magnetic rigidity ranges covered in the experiments, as mentioned in section 2.

It is noteworthy that in both reactions the DIT and CoMD primary distributions yield similar shapes and tendencies especially for atomic numbers near the projectile (Z=34–36). This, however, changes notably after the de-excitation.

On the (25 MeV/nucleon) ^{86}Kr +^{64}Ni reaction for Z = 36–34, both filtered DIT and CoMD calculations describe the data in an overall good way. Nevertheless, for Z = 33–31 the DIT calculation seems to describe the experimental data better than the CoMD calculation.

On the (25 MeV/nucleon) ^{86}Kr +^{124}Sn reaction for Z = 36–34, we observe similar tendencies on both filtered DIT and CoMD calculations. However, the opposite is true for Z = 33–31 where the CoMD calculation seems to describe the experimental data equally well as DIT.

Generally, as for both the DIT and CoMD models, the filtered calculations seem to describe the experimental data. On the one hand, the CoMD calculation seems to describe better the proton rich side of the distributions and on

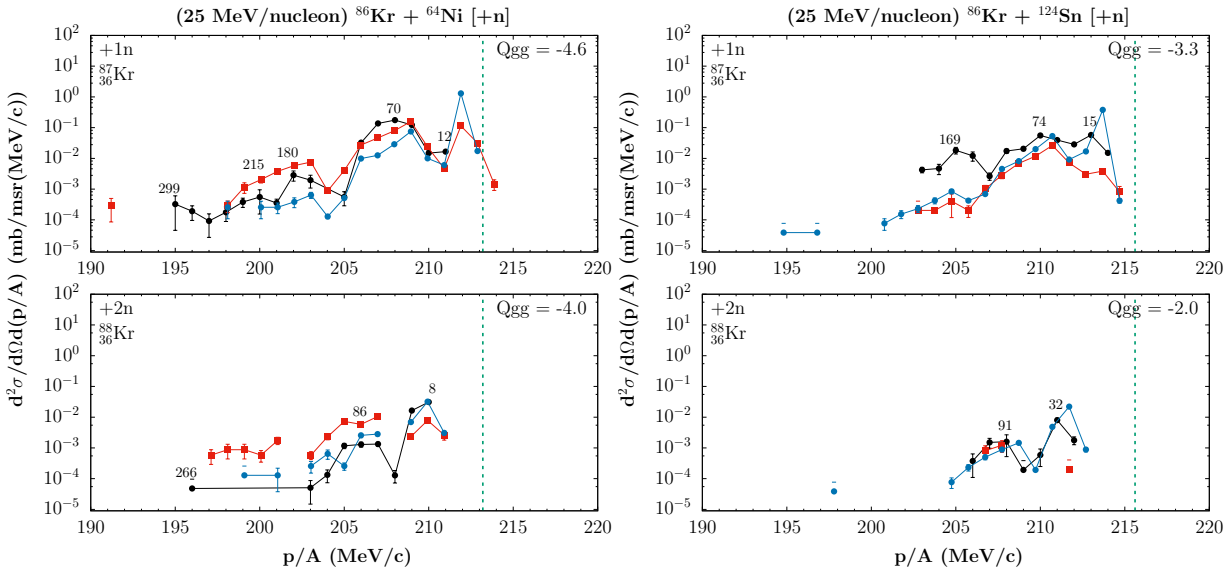

Figure 3. Momentum per nucleon distributions of ejectiles from neutron pickup channels of (25 MeV/nucleon) ^{86}Kr + ^{64}Ni (left) and (25 MeV/nucleon) ^{86}Kr + ^{124}Sn (right). Experimental data: closed (black) circles. Vertical dashed (green) line: p/A of the beam. Numbers above peaks: total excitation energy of QP–QT system in MeV. Qgg: Ground-to-ground state Q-value in MeV. DIT calculations: closed (blue) circles. CoMD calculations: closed (red) squares.

the other hand, the neutron rich side is better described by the DIT calculations. Overall, the DIT calculations seem to describe the neutron rich side in the most effective way for both systems studied.

4.2 Proton Removal Channels

In regards to the reaction channels that produce neutron rich fragments, in Fig. 2, we present the channels of the removal of one up to four protons for the (25 MeV/nucleon) ^{86}Kr + ^{64}Ni (left panel) and the (25 MeV/nucleon) ^{86}Kr + ^{124}Sn (right panel) reactions. We point out that the p/A distributions correspond to the angular ranges of $\Delta\theta = 1.0° - 2.7°$ and $\Delta\theta = 2.7° - 5.4°$ that are inside the grazing angles of the ^{86}Kr + ^{64}Ni and ^{86}Kr + ^{124}Sn, respectively. The vertical axis gives differential cross section $\frac{d^2\sigma}{d\Omega d(p/A)}$ in units of $\frac{mb}{msr(MeV/c)}$. The experimental distributions have a characteristic shape that is similar to the channels that we will discuss in the following sections. The distributions have a quasielastic peak near (just below) the p/A value of the beam (exiting each target), shown by the vertical (green) dashed line, and an extended dissipative region at lower p/A values. The "valleys" that are present in the data originate from excluded magnetic rigidity regions corresponding to elastically scattered projectiles at their most intense charged states. Finally, the numbers above some peaks express the total excitation energy of the di-nuclear system (quasiprojectile – quasitarget) in MeV, obtained from binary kinematics using the corresponding p/A values and assuming no neutron emission. In both distributions the experimental data are represented by black symbols, DIT calculations by blue symbols, and CoMD calculations by red symbols.

For the Kr + Ni system, the DIT calculations seem to underestimate the QE peak, but provide with a better description of the dissipative peaks. This is true especially on the -2p channel. The CoMD calculations overall describe the experimental distributions, the QE peaks on the -1p and -3p channels, in particular.

For the Kr + Sn system on the other hand, both calculations seem to perfrom reasonably well. It is noteworthy that both calculations have reached the -4p channel for the Kr + Ni system and that only the DIT has reached this channel for Kr + Sn. These channels correspond to an estimated cross section below 10 μb for both systems (see Fig. 1). Indeed, to reach very low cross sections we need high statistics in our Monte Carlo calculations. We note that, the current DIT calculation corresponds to three million events and the CoMD to one million events for both Kr + Ni and Kr + Sn systems.

4.3 Neutron Pickup Channels

In Fig. 3, we present channels of the pickup of one and two neutrons. As before, the left panels are p/A distributions for the Kr + Ni system and the right panels for the Kr + Sn system. For both the the Kr + Ni and Kr + Sn systems, the DIT and CoMD calculations seem to follow the trends of the experimental data to a large extent both in the QE and the dissipative region.

4.4 Multiple Charge Exchange Channels

In Fig. 4, we present the observed multiple charge exchange channels in which there is a net removal of protons and addition of neutrons to the projectile. Interestingly, these channels lead effectively to very neutron rich isotopes. The DIT and CoMD calculations appear to describe the trend of the data in some of the channels. More specifically, in the single charge exchange (SCE) channel

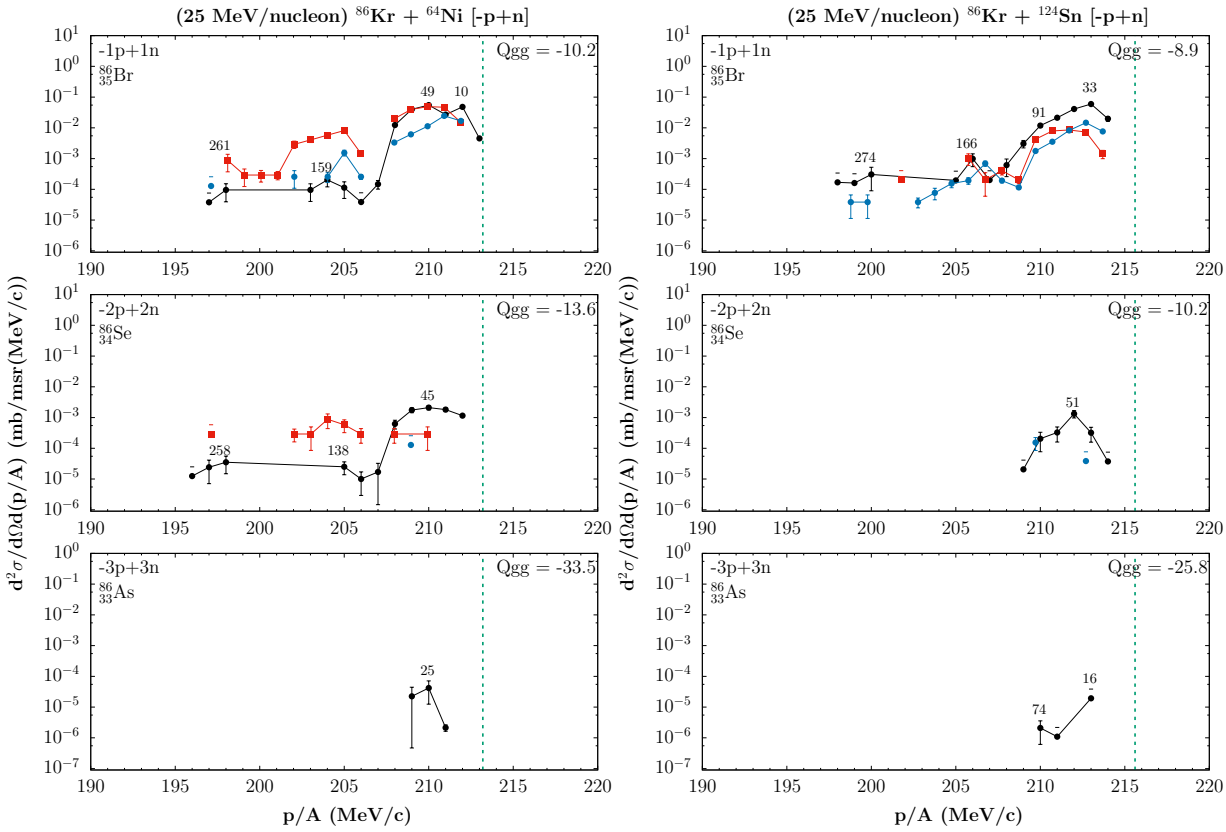

Figure 4. Momentum per nucleon distributions of ejectiles from multiple charge exchange channels of (25 MeV/nucleon) ^{86}Kr + ^{64}Ni (left) and (25 MeV/nucleon) ^{86}Kr + ^{124}Sn (right). Experimental data: closed (black) circles. Vertical dashed (green) line: p/A of the beam. Numbers above peaks: total excitation energy of QP–QT system in MeV. Qgg: Ground-to-ground state Q-value in MeV. DIT calculations: closed (blue) circles. CoMD calculations: closed (red) squares.

-1p+1n, for the Kr + Ni system, the CoMD calculation nicely describes the QE part and the DIT is lower; for the Kr + Sn system both calculations yield similar results that lie below the data in the QE part.

For the double charge exchange (DCE) channels -2p+2n, the DIT calculation gives 1-2 points below the data in the QE part for both Kr + Ni and Kr + Sn systems, whereas the CoMD calculation provides results only for the Kr + Ni system lying below the data in the QE part (and above the data in the dissipative part, as in the SCE channel).

Finally for the triple charge exchange (TCE) channel -3p+3n, we have no calculation points for both reactions in the p/A distributions (and in the yield distributions, Fig. 1), apparently due to inadequate statistics of our Monte Carlo calculations to describe this very distant channel (with experimental cross section of about 0.5 μb, according to Fig. 1). Considering the complicated nature of the multiple charge exchange channels and the observation that our DIT calculations reach (but highly underestimate) the DCE channel for both systems, we speculate that additional mechanisms beyond independent nucleon exchange (including pair transfer and/or meson-mediated charge exchange) may be present, motivating further dedicated study of these channels.

5 Conclusions

This article describes our theoretical study of peripheral collisions of a ^{86}Kr projectile at 25 MeV/nucleon and targets of ^{64}Ni and ^{124}Sn. We focused on the neutron rich ejectiles from these reactions, data of which were obtained with the MARS spectrometer at Texas A&M University. Using the original data, we extracted experimental yield distributions and momentum per nucleon distributions in an effort to elaborate on our study of the reaction mechanisms that lead to the production of very neutron rich isotopes. We compared these experimental distributions with detailed calculations with the DIT and CoMD models that offered an overall description of the trends of experimental data.

From the study of the proton removal, neutron pickup and multiple charge exchange reaction channels, DIT and CoMD calculations give an overall fair reproduction of most of the data. We are performing further systematic examination of the model parameters and search for potential improvements. An overall conclusion from the present study at 25 MeV/nucleon is that the mechanism of independent nucleon exchange, as implemented phenomenologically in the DIT model and microscopically in the CoMD model, appears to be a major contributor to the observed distributions of neutron rich nuclides near the projectile. We point out that possible contributions

of mechanisms beyond independent nucleon exchange including pair transfer [13], cluster transfer and meson mediated charge exchange [14] are of special interest and require detailed calculations with appropriate models. Especially the last mechanism may have important contribution on the channels of multiple charge exchange in the present data that appear to be under-predicted or unreachable with our present models.

As for our upcoming steps, we plan to continue the systematic study of multinucleon transfer reactions in the Fermi energy region, especially in the reactions with a ^{86}Kr projectile at 15 MeV/nucleon with ^{64}Ni and ^{124}Sn targets (a preliminary study is already presented in [7]). Moreover, we will continue with detailed efforts on the reconstruction of the excitation energy distributions [15] hoping to gain further insight into the details of the reaction mechanisms. In closing, through our ongoing endeavor in the study of multinucleon transfer in the Fermi energy region, we expect to obtain valuable information on the reaction mechanisms and improve our theoretical model framework of peripheral reactions in this energy regime. From a practical standpoint, we can apply the obtained experience toward the production and study of neutron rich nuclides.

References

[1] J. Diklić, S. Szilner, L. Corradi, T. Mijatović, et al., Transfer reactions in ^{206}Pb+^{118}Sn: From quasielastic to deep-inelastic processes, Phys. Rev. C **107**, 014619 (2023). https://link.aps.org/doi/10.1103/PhysRevC.107.014619

[2] T. Mijatović, Multinucleon transfer reactions: a mini-review of recent advances, Front. Phys **10**, 965198 (2022). https://doi.org/10.3389/fphy.2022.965198

[3] G.A Souliotis, M Veselsky, G Chubarian, L Trache, A Keksis, et al., Enhanced production of neutron-rich rare isotopes in the reaction of 25 MeV/nucleon ^{86}Kr on ^{64}Ni, Phys. Lett. B **543**, 163 (2002). https://doi.org/10.1016/S0370-2693(02)02459-0

[4] G. A. Souliotis, M. Veselsky, G. Chubarian, L. Trache, A. Keksis, et al., Enhanced Production of Neutron-Rich Rare Isotopes in Peripheral Collisions at Fermi Energies, Phys. Rev. Lett. **91**, 022701 (2003). https://doi.org/10.1016/j.nuclphysa.2011.09.016

[5] G. A. Souliotis, M. Veselsky, S. Galanopoulos, M. Jandel, Z. Kohley, et al., Approaching neutron-rich nuclei toward the r-process path in peripheral heavy-ion collisions at 15 MeV/nucleon, Phys. Rev. C **84**, 064607 (2011). https://doi.org/10.1103/PhysRevC.84.064607

[6] O. Fasoula, G. A. Souliotis, Y. K. Kwon, K. Tsoo, M. Veselsky, et al., Production cross sections and angular distributions of neutron-rich rare isotopes from 15 MeV/nucleon Kr-induced collisions: toward the r-process path, accessible at: https://arxiv.org/pdf/2103.10688.pdf

[7] O. Fasoula, G. A. Souliotis, S. Koulouris, K. Palli, M. Veselsky, et al., etailed Study of the Reaction Mechanisms of ^{86}Kr + ^{64}Ni at 15 MeV/nucleon, HNPS Advances in Nuclear Physics **30**, 181-184 (2024). https://doi.org/10.12681/hnpsanp.6271

[8] S. Koulouris, G. A. Souliotis, F. Cappuzzello, D. Carbone, A. Pakou, et al., Study of multinucleon transfer channels from ^{70}Zn (15 MeV/nucleon) + ^{64}Ni collisions, Phys. Rev. C **108**, 044612, (2023). https://doi.org/10.1103/PhysRevC.108.044612

[9] K. Palli, G. A. Souliotis, I. Dimitropoulos, T. Depastas, O. Fasoula, S. Koulouris, M. Veselsky, S. J. Yennello, and A. Bonasera, Microscopic description of multinucleon transfer in ^{40}Ar + ^{64}Ni collisions at 15 MeV/nucleon. EPJ Web Conf. **252**, 07002 (2021). https://doi.org/10.1051/epjconf/202125207002

[10] L. Tassan-Got, C. Stephan, Deep inelastic transfers: a way to dissipate energy and angular momentum for reactions in the Fermi energy domain, Nucl. Phys. A **524**, 121 (1991). https://doi.org/10.1016/0375-9474(91)90019-3

[11] M. Papa, T. Maruyama, A. Bonasera, Constraint molecular dynamics approach to fermionic systems, Phys. Rev. C **64**, 024612 (2001). https://doi.org/10.1103/PhysRevC.64.024612

[12] R. J. Charity, M. A. McMahan, G. J. Wozniak, R. J. McDonald, L. G. Moretto, et al., Systematics of complex fragment emission in niobium-induced reactions, Nucl. Phys. A **483**, 371 (1988). https://doi.org/10.1016/0375-9474(88)90542-8

[13] C. Agodi, G. Giuliani, F. Cappuzzello, A. Bonasera, D. Carbone, et al., Analysis of pairing correlations in neutron transfer reactions and comparison to the constrained molecular dynamics model, Phys. Rev. C **97**, 034616 (2018). https://doi.org/10.1103/PhysRevC.97.034616

[14] H. Lenske, F. Cappuzzello, M. Cavallaro, M. Colonna, Heavy ion charge exchange reactions as probes for nuclear β-decay, Progress in Particle and Nuclear Physics **109**, 103716 (2019). https://doi.org/10.1016/j.ppnp.2019.103716

[15] G. A. Souliotis, P. N. Fountas, M. Veselsky, S. Galanopoulos, Z. Kohley, et al., Isoscaling of heavy projectile residues and N/Z equilibration in peripheral heavy-ion collisions below the Fermi energy. Phys. Rev. C **90**, 064612 (2014). https://doi.org/10.1103/PhysRevC.90.064612